An Image Driven Biophysical Model of Tumor Cell Proliferation

David A Hormuth,II[1,2], Nkiruka C Atuegwu[2], and Thomas E Yankeelov[1,2]
[1]*Biomedical Engineering, Vanderbilt University, Nashville, TN, United States,* [2]*Institute of Imaging Science, Vanderbilt University, Nashville, TN, United States*

TARGET AUDIENCE: Those studying 1) brain tumor development, and 2) mathematical modeling of tumor growth.

PURPOSE: Recent advances in MRI and PET have increased the availabilty of noninvasive measurements of the molecular, cellular, and physiological characteristics of tumors. It may be possible to incorporate these measureable tumor characteristics into a realistic biophysical model that can then be used to predict tumor growth and therapy response on an individual basis. Typical mathematical models of tumor growth require many assumptions on model parameters as they are extraordinarily difficult to directly measure in an intact organism. Here we incorporate MRI and PET data from rats into a model of tumor growth.

METHODS: Six Sprague-Dawley rats with C6 gliosarcomas were imaged with diffusion weighted MRI (DW-MRI) and dynamic contrast enhanced MRI (DCE-MRI) on days 9, 10, 11, 13, 15, and 17, and with ^{18}F-FDG-PET on days 9, 15, and 17. Cell number was estimated from ADC maps as previously described[1]. ADC maps were also used to calculate tumor cell diffusion (D_{TC}) and proliferation ($k_{p,TC}$) following the method by Ellingson *et al*[2]. Imaging data from the central tumor slice was then incorporated into a model (see **Figure**) consisting of two coupled partial differential equations, describing the time dependent changes in tumor cell number and glucose concentration[3,4], which was then solved using the finite difference method. Eq. (1) incorporates random tumor cell (N_{TC}) movement, logistic growth, directed movement along vasculature (N_{EC}), and a death term. v_p (estimated form DCE-MRI data) provided N_{EC} within the tumor, whereas elsewhere the average v_p of the healthy brain was assigned. When $C_g(\bar{x},t)$ (estimated by the FDG-PET data) was above $C_{g,critical}$, cells proliferated at rate $k_{p,TC}$; whereas, when $C_g(\bar{x},t) < C_{g,critical}$, cells ceased to proliferate ($k_{p,TC} = 0$) and underwent apoptosis at a rate $k_{d,TC}$. Glucose concentration (C_g), represented in Eq. (2), varies spatially depending on its diffusion through tissue, consumption by tumors cells (T_g), and delivery (estimated by K^{trans} from the DCE-MRI data) by the local vasculature (F_g). The model was initialized with cell number data from day 9, and $k_{p,TC}$ and D_{TC} maps derived from days 9, 10, and 11. Agreement between predicted and observed tumor growth, as described by cell number and tumor volume, was assessed with the Pearson correlation coefficient (PCC) and the concordance correlation coefficient (CCC).

$$\frac{\partial N_{TC}(\bar{x},t)}{\partial t} = \nabla \bullet [D_{TC}\nabla N_{TC}(\bar{x},t)] + k_{p,TC}(\bar{x},t)N_{TC}(\bar{x},t)\left(1-\frac{N_{TC}(\bar{x},t)}{\theta}\right) - \nabla \bullet [\chi_{TC}N_{TC}(\bar{x},t)\nabla N_{EC}(\bar{x},t)] - k_{d,TC}(\bar{x},t)N_{TC}(\bar{x},t) \quad (1)$$

$$\frac{\partial C_G(\bar{x},t)}{\partial t} = \nabla \bullet [D_G \nabla C_G(\bar{x},t)] - T_G(\bar{x},t) + F_G(\bar{x},t) \quad (2)$$

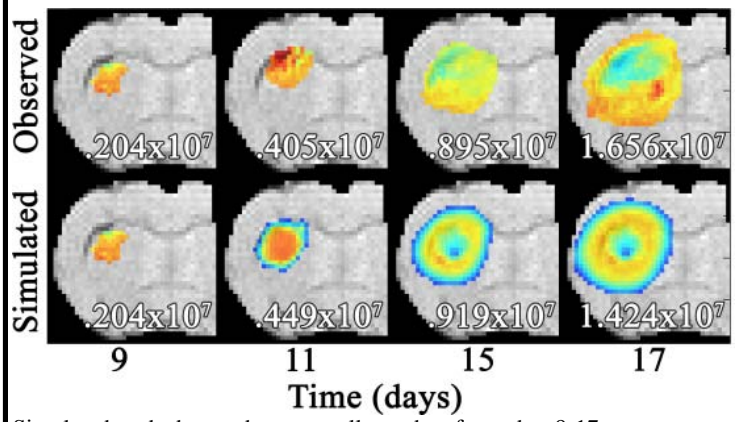

Simulated and observed tumor cell number from day 9-17 post tumor implantation. Tumor cell growth was modeled using an equation for tumor cell number (Eq. 1) and an equation describing glucose concentration (Eq.2)

RESULTS: Simulated and observed tumor growth for the central tumor slice is shown in the figure. Predicted and observed cell number and tumor volume resulted in PCCs of 0.994 and 0.989, respectively, and CCCs of 0.749 and 0.736, respectively. Of note is that a necrotic core is present in both simulated and observed tumor growths on day 15 and 17.

DISCUSSION: The high PCCs suggest a strong linear relationship between predicted and observed values. Early tumor cell growth is in strong agreement; however, between day 15 and 17 cell death is overestimated in the simulation. Importantly, the predicted tumor resulted in a necrotic region which was also observed *in vivo*. Ongoing work is focused on expanding the model described in the figure to include both vascular (from DCE-MRI data) and oxygen (from quantitative BOLD data) status which we hypothesize will increase the accuracy of the modeling predictions.

CONCLUSION: Preliminary results indicate the potential to predict *in vivo* tumor growth using imaging data obtained early in a tumor's growth cycle. Incorporating subject specific imaging data into appropriate models of tumor growth will allow direct comparison between predicted and observed tumor characteristics.

REFERENCES:

1.Atuegwu NC, Gore JC, Yankeelov TE. *Physics in Medicine and Biology.* May 7 2010;55(9):2429-2449.**2.**Ellingson BM, LaViolette PS, Rand SD, et al. *Magn Reson Med.* Apr 2011;65(4):1132-1144.**3.**Gerlee P, Anderson ARA. *J Theor Biol.* 2008;250(4):705-722.
4.Cai Y, Xu SX, Wu J, Long Q. C *J Theor Biol.* Jun 21 2011;279(1):90-101.

ACKNOWLEDGEMENTS: NCI-P30CA068485, NCI-R01CA138599, and NCI-R25CA136440.